Current-Driven Magnetization Reversal and Spin-Wave Excitations in Co/Cu/Co Pillars

J. A. Katine, F. J. Albert, and R. A. Buhrman

School of Applied and Engineering Physics, Cornell University, Ithaca, New York 14853

E. B. Myers and D. C. Ralph

Laboratory of Atomic and Solid State Physics, Cornell University, Ithaca, New York 14853

Using thin film pillars $\sim$100 nm in diameter, containing two Co layers of different thicknesses separated by a Cu spacer, we examine the process by which the scattering from the ferromagnetic layers of spin-polarized currents flowing perpendicular to the layers causes controlled reversal of the moment direction in the thin Co layer. The well-defined geometry permits a quantitative analysis of this spin-transfer effect, allowing tests of competing theories for the mechanism and also new insight concerning magnetic damping. When large magnetic fields are applied, the spin-polarized current no longer fully reverses the magnetic moment, but instead stimulates spin-wave excitations.

Theoretical calculations have recently predicted that when a spin-polarized current passes through a ferromagnetic conductor, the transfer of angular momentum from the polarized current exerts a torque on the magnetic moment of the conductor. At sufficiently high current densities, J, this interaction is expected to stimulate spin-wave excitations [1–3] or to possibly flip the magnetic moment of an individual domain [2]. Evidence for spin-transfer-induced excitations has been reported previously in point-contact measurements of Cu/Co multilayers [4,5] and nickel wires [6], and spin-transfer-driven moment reversals have been reported in manganite junctions [7] and point contacts [5]. Utilizing a geometry specifically tailored to emphasize spin transfer—lithographically patterned pillars consisting of two Co layers of different thicknesses separated by a paramagnetic Cu layer spacer—we report here the clearest signatures to date of spin-transfer effects. Furthermore, since the pillar devices are a well-controlled geometry with a known thickness and diameter, they facilitate the first quantitative study of the spin-transfer effect and allow tests of the theoretical models describing the phenomenon. With these devices we confirm the results of [5] that, in low applied magnetic fields H, spin-polarized electrons flowing from the thin Co layer to the thick layer can switch the moment of the thin layer antiparallel to the thick-layer moment, while a reversed current produces a switch back to the parallel orientation. In the point contact study [5], which involved continuous ferromagnetic layers, extreme ($\sim 10^9$ A/cm^2) current densities were required to reverse the magnetization direction of a localized domain. In our pillar geometry, however, the spin-polarized current is incident on an isolated ferromagnetic particle; hence, the domain which reverses is not exchange coupled to a continuous magnetic layer. The reorientations therefore occur at far more modest current densities ($<10^8$ A/cm^2) than in [5]. In the high field regime, the spin-transfer effect cannot produce a full reversal of the thin-layer moment,

but gives instead a clean signal of a precessing spin-wave excitation. In contrast to the previous mechanical point contact study [4], quantitative measurements here of the spin-wave signal show good agreement with theory using established magnetic parameters of Co.

Figure 1 is a schematic representation of the pillar device. A number of groups [8–11] have used lithographic patterning to perform CPP (current perpendicular-to-plane) measurements on magnetic multilayers exhibiting giant magnetoresistance (GMR). Here we use GMR as a probe of the relative orientation of the two Co layers, in pillars much narrower than those previously made. We begin fabrication by sputtering 1200 Å Cu/100 Å Co/ 60 Å Cu/25 Å Co/150 Å Cu/30 Å Pt/600 Å Au onto an oxidized Si substrate. The difference in thickness for the Co layers allows the magnetization direction of the thicker layer to be held fixed, so that the polarity of the current bias associated with the spin-transfer excitations in the thinner layer can be determined. Electron beam lithography, evaporation, and lift-off are used to pattern $\sim$100 nm diameter, 500 Å thick Cr dots on top of the sputtered film. These serve as a mask during an ion milling step that etches through the bottom Co layer.
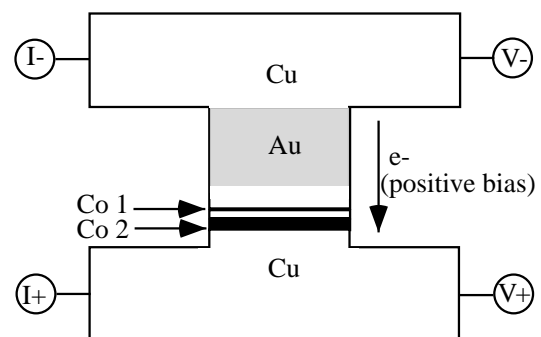

FIG. 1. Schematic of pillar device with Co (dark) layers separated by a 60 Å Cu (light) layer. At positive bias, electrons flow from the thin (1) to the thick (2) Co layer.

The final device diameter is 130 ± 30 nm. Following planarization with polyimide, reactive ion etching and photolithography are used to uncover the Au surface of the pillar, and pattern the top leads.

Figure 2a shows graphs of the room temperature differential resistance dV/dI vs I in one pillar, taken with magnetic fields H of 1200 and 1600 Oe applied in the plane of the film. H fixes the magnetization of the thick Co layer, $\vec{M}_2$, and also helps prevent the formation of domains within the layers. dV/dI is measured using lock-in techniques with a 10 μA ac excitation, and the dc resistance R_{dc} is monitored simultaneously. Consistent with [5], we define positive bias such that electrons flow from the thin Co layer to the thick Co layer. Examining the 1200 Oe data, we begin for $I = 0$ with the device in the low resistance state. I is first swept positive and dV/dI (and R_{dc}, not pictured) increases in two discrete jumps at 9 and 13 mA, corresponding to $J = 0.7$ and 1.0×10^8 A/cm^2, respectively. The curve is hysteretic, with the device remaining in this high R state until the current is swept to negative values where it returns to the low R orientation in a single jump. In addition to the jumps, there is a gradual rise in R with increasing bias due to growth of electron-magnon and electron-phonon scattering. We attribute the jumps in R to changes in the relative alignment of the magnetization of the Co layers, with the low resistance state reflecting parallel alignment of the layer magnetizations, and the high resistance state corresponding to antiparallel alignment. The 73 mΩ total difference in R is very close
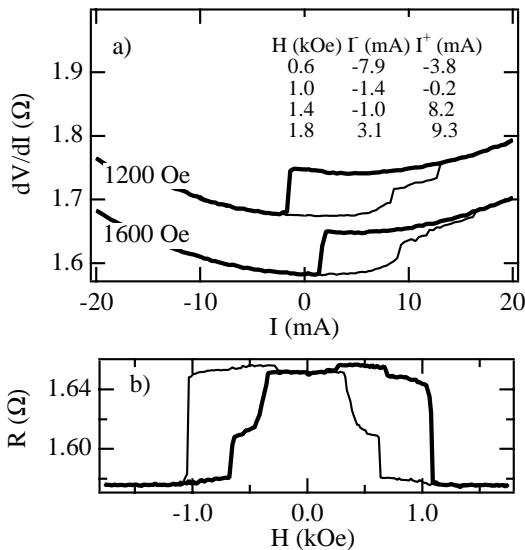

FIG. 2. (a) dV/dI of a pillar device exhibits hysteretic jumps as the current is swept. The current sweeps begin at zero; light and dark lines indicate increasing and decreasing current, respectively. The traces lie on top of one another at high bias, so the 1200 Oe trace has been offset vertically. The inset table lists the critical currents at which the device begins to depart from the fully parallel configuration (I^+) and begins to return to the fully aligned state (I^-). (b) Zero-bias magnetoresistive hysteresis loop for the same sample.

to that observed for magnetization realignment as a function of H at $I = 0$, shown in Fig. 2b.

From Fig. 2b, we note that for $I = 0$ the sample returns to the high-resistance antiparallel state before the sign of H is reversed, indicating the presence of antiferromagnetic coupling between the layers. Although exchange coupling through the 60 Å Cu layer should be quite weak, in a narrow pillar geometry antiferromagnetic alignment may be created by the presence of magnetostatic edge charges, evidence of which has been reported in significantly wider multilayer pillars [12]. We calculate that a magnetostatic interaction H_{ex} of roughly 1000 Oe should be felt by the edge of thinner Co layer in our geometry. Since R is only a measure of the relative alignment of the magnetization of the two layers, when a plateau is observed in the magnetoresistance at some intermediate value (e.g., at ± 500 Oe in Fig. 2b), we do not know if it is because a layer is essentially single domain and has had its magnetization rotate into a quasistable configuration, or if it is because layer 1 contains two domains with different coercive fields. The nature of the two discrete upward jumps in resistance as a function of I in Fig. 2a is similarly ambiguous.

That a sufficiently large spin-polarized current can flip the magnetization of an isolated particle was predicted by Slonczewski by incorporating spin-transfer effects into the Landau-Lifshitz equation [2]. Adapting Slonczewski's argument to our geometry, consider a simplified model of the pillar devices in which the thin Co layers lie in the a-c plane with the b axis perpendicular to the thin film. H is directed along the c axis which is also the axis of a uniaxial anisotropy term of strength H_{an}. If we assume that the magnetization of layer 2 is fixed and that layer 1 is a single domain particle of volume V and total spin $\vec{S}$ ($S \equiv |\vec{S}| = MV/\gamma\hbar$, where $M = 1420$ emu/cm^3 for Co and γ is the gyromagnetic ratio), we then have

$$\frac{d\hat{s}}{dt} = \hat{s} \times \left\{ \gamma[H_{eff}\hat{c} - 4\pi M(\hat{s} \cdot \hat{b})\hat{b}] \right.$$
$$\left. - \alpha\frac{d\hat{s}}{dt} - \frac{Ig(\theta)}{eS}\hat{c} \times \hat{s} \right\}, \qquad (1)$$

where $H_{eff} = H_{an}\cos(\theta) + H - H_{ex}$ is the sum of the anisotropy, applied, and exchange (but not demagnetizing) fields, θ represents the angle between the magnetization vectors of layers 1 and 2, and the second term on the right of the equation takes into account the demagnetization effect. The coefficient α is the phenomenological Gilbert damping parameter. The final term incorporates spin-transfer effects, in which $g(\theta)$ is a coefficient that depends on the polarization of the electrons, and is calculated to increase monotonically with θ [2]. In the absence of the spin-transfer term and damping, the solution of this equation is elliptical precession of $\hat{s}$ about the c axis with $S_a = A\cos(\omega t)$, $S_b = -A(\gamma H_{eff}/\omega)\sin(\omega t)$, and $\omega^2 = \gamma^2 H_{eff}(H_{eff} + 4\pi M)$. Damping causes the

amplitude A of the precession to decay with time, while depending on the sign of I, the spin-transfer term can amplify or attenuate the precession amplitude. For small amplitudes of precession A about $\theta = 0$, the time-averaged rate of change in the total energy is

$$\left\langle \frac{dE}{dt} \right\rangle \approx A^2 \frac{H_{\text{eff}} M}{S^2}$$
$$\times \{-\alpha\gamma[H_{\text{eff}} + 2\pi M] + Ig(\theta)/(eS)\}. \quad (2)$$

Near $\theta = 0$, negative values of $\langle dE/dt \rangle$ indicate a decay of the spin precession toward $\theta = 0$. A similar expression may be derived near $\theta = \pi$. If we begin near parallel alignment ($\theta \approx 0$) and ramp the current, then that alignment remains stable until $I > I_c^+ = \alpha\gamma eS[H_{\text{eff}}(0) + 2\pi M]/g(0)$, after which $\theta = \pi$ is the only stable configuration. Conversely, if the applied field is not too large ($|H - H_{\text{ex}}| < H_{\text{an}} + 2\pi M$) and if the device is in the antiparallel alignment, it will remain there until the current decreases below $I_c^- = \alpha\gamma eS[H_{\text{eff}}(\pi) - 2\pi M]/g(\pi)$, when it will switch into the parallel configuration.

This model correctly predicts the symmetries of hysteretic switching observed in our devices and in previous point contact studies [5]. The dependence of the switching on the direction of I is strong evidence that a spin-transfer mechanism and not the oersted fields created by the current flow is responsible for the effect. As recent experiments in multilayer pillars have demonstrated [13], for larger sample diameters these oersted fields can create vortex magnetization states, but such effects are symmetric in regards to the direction of current flow. Since an applied field favors parallel alignment, the spin-transfer model predicts that increasing H should make both I_c^- and I_c^+ more positive. This is indeed the case in our devices as illustrated by the inset table in Fig. 2a where we list, for different values of the applied field, the critical currents I^+ at which the device starts to leave the fully parallel state and the currents I^- at which the device begins to return to parallel alignment. Lower values of H are not included since the well-ordered switching behavior shown in Fig. 2a is not present for $H \leq 500$ Oe. This is not surprising since the assumption that the thick Co layer is a single domain of fixed magnetization is likely no longer valid.

Although the values of H_{an} and H_{ex} are not precisely known in our devices, the $2\pi M$ term should dominate their contributions to the critical switching currents. Assuming a Co polarization of 38% [14] and a damping coefficient $\alpha = 0.007$ determined from ferromagnetic resonance studies of Co [15], the predicted separation between I^+ and I^- should be approximately 4 mA, in good agreement with the results in Fig. 2a. A further comparison can be made to the predicted critical currents by examining how I^+ and I^- change relative to H. From the inset in Fig. 2a, we see that a change in H of 1 kOe increases I^+ by approximately 12 mA, and I^- by 5 mA. In our simple model, however, the predicted change in I_c^+ with H is roughly 0.5 mA/kOe, more than an order

of magnitude below the values seen in our devices. Of course, the magnetic transitions of the thin Co layer are, in moderate magnetic fields, likely to be more complicated than the uniform rotation of a single domain particle assumed in the model. In particular, the gradual onset of the transition and the multiplateau features often observed suggest that multiple domains and possibly domain wall motion may be involved. As H varies, it is reasonable to expect that any such domain formation within the layers would be affected, so it is not surprising that large jumps in I^+ and I^- are observed.

As H is increased above 2.3 kOe, discrete switching behavior is no longer observed. Instead spikes in dV/dI emerge as shown in Fig. 3a. Figure 3b shows the corresponding R_{dc} traces. The data presented were taken at 4.2 K, though the spikes were also present at 300 K. Here H was applied in the plane of the film, but similar results were obtained for high H perpendicular to the
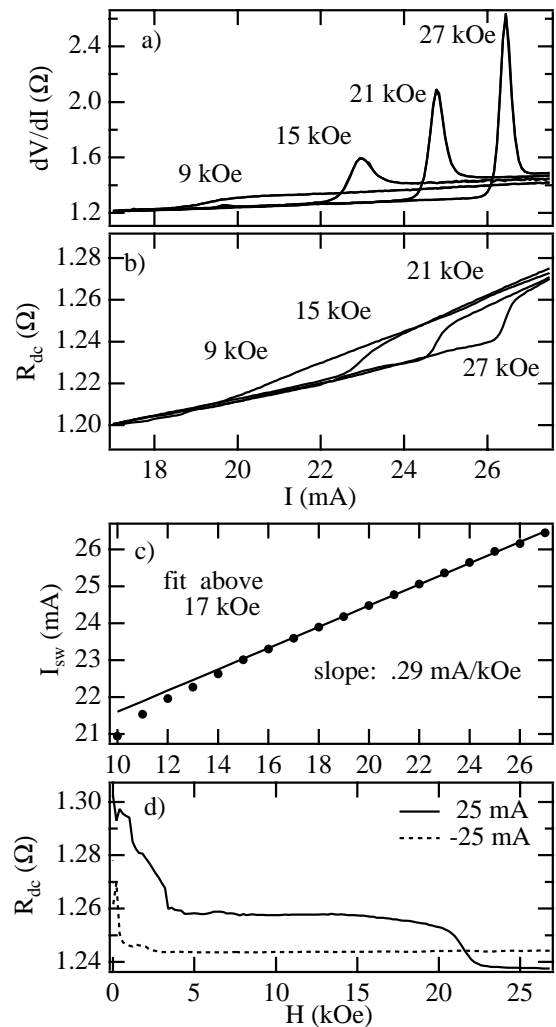
FIG. 3. (a) As H increases, the spike in the dV/dI traces occurs at a larger critical current I_{sw}. (b) R_{dc} traces of the same measurements as in (a). (c) Plot of I_{sw} vs H. (d) R_{dc} vs H with a 25 mA bias current applied in both directions.

plane. These data strongly resemble those observed in point contact studies of unbounded multilayer films [4,5]. Figure 3d plots R_{dc} vs H with constant bias currents of ± 25 mA. For the $+25$ mA curve, the resistance maximum near $H = 0$ demonstrates antiparallel alignment, and the low-resistance region $H > 22$ kOe is for parallel alignment. The plateau between 5 and 20 kOe for the $+25$ mA curve, where the dc resistance has an intermediate value, corresponds to the region of increased resistance beyond the peaks in the dV/dI vs I plots in Fig. 3a. We can therefore argue that the spikes in Fig. 3a do not denote a full reversal of the thin-layer moment, but must correspond to a precessing spin-wave state in between parallel and antiparallel alignment.

To excite the spin-wave mode the injected current must provide a torque deflecting the moment of the thin layer away from the aligned configuration. As discussed earlier, this corresponds to a positive bias in our devices. We have studied several dozen samples and always observe the spikes in dV/dI on the positive side. In many instances, there are several spikes present which may be the result of inhomogeneities within the samples. Unlike point contacts where similar spikes were observed previously, the current density in the pillar devices is constant through both layers, which makes clear the intrinsic asymmetry of the phenomenon. On the negative bias side, we have performed measurements out to -80 mA ($J = 6 \times 10^8$ A/cm^2), without ever observing spikes in dV/dI.

Two different mechanisms explaining how bias currents may generate spin waves have been proposed. Berger argues that spin waves can occur once $e\Delta\mu = h\nu$, where $\Delta\mu$ is the spin splitting of the chemical potential and ν is the ferromagnetic resonance frequency [1], while Slonczewski [16] has approached the spin-wave excitations using the same spin-transfer framework applied to calculate I_c^+. In this approach the existence of a stable spin-precessing mode is somewhat curious, because the solution of the Landau-Lifshitz equation for $H \gg 2\pi M$ does not have stable states other than $\theta = 0$ or π, as long as $g(\theta)$ increases monotonically with θ and α is a constant independent of θ. However, the assumption that α is constant is the result of a small angle expansion [17]. Keeping next-to-leading-order terms, the argument in [17] predicts $\alpha \propto [1 - \cos(\theta)]/\sin^2(\theta)$, which is sufficient to stabilize a precessing spin-wave mode at large H. Other nonlinear effects might also contribute to $\alpha(\theta)$. Although a potential field-independent offset may exist in the pillar geometry, the critical current I_{sw} required to excite the spin-wave mode at large H in the Slonczewski model [16] is otherwise identical to I_c^+ calculated above. If we use the value of 0.14 for $g(0)$ calculated using a WKB approxi-

mation [2], the slope of 0.29 mA/kOe in Fig. 3c corresponds to $\alpha = 0.005$. This value agrees quite well with the previously quoted α of 0.007 measured in ferromagnetic resonance experiments on Co films [15]. In contrast, in previous point contact measurements, where a spin wave was induced in a magnetic region exchange coupled to an unbounded film, damping coefficients 10–50 times larger were necessary to explain how I_{sw} scaled with increasing field [4,5].

In summary, we have fabricated narrow pillars containing Co/Cu/Co layers. Using the GMR effect as a probe, we have demonstrated that for low H an applied current can be used to controllably flip the relative magnetization alignment of the Co layers, in general accord with spin-transfer theory. For larger H, a current bias of the proper polarity can excite uniformly precessing spin-wave modes, and in this regime we find excellent quantitative agreement between our experimental data and the spin-transfer theory, particularly with respect to the damping parameter α. The fabrication technique developed for these CPP measurements is quite versatile and may be applied to a large number of materials systems whose interfacial transport properties have previously been very difficult to probe.

[1] L. Berger, Phys. Rev. B **54**, 9353 (1996).
[2] J. Slonczewski, J. Magn. Magn. Mater. **159**, L1 (1996).
[3] Ya. B. Bazaliy, B. A. Jones, and S.-C. Zhang, Phys. Rev. B **57**, R3213 (1998).
[4] M. Tsoi *et al.,* Phys. Rev. Lett. **80**, 4281 (1998); **81**, 493(E) (1998).
[5] E. B. Myers *et al.,* Science **285**, 867 (1999).
[6] J.-E. Wegrowe *et al.,* Europhys. Lett. **45**, 626 (1999).
[7] J. Z. Sun, J. Magn. Magn. Mater. **202**, 157 (1999).
[8] M. A. M. Gijs *et al.,* Appl. Phys. Lett. **63**, 111 (1993).
[9] W. Vavra *et al.,* Appl. Phys. Lett. **66**, 2579 (1995).
[10] K. Bussmann *et al.,* IEEE Trans. Magn. **34**, 924 (1998).
[11] J. P. Spallas *et al.,* IEEE Trans. Magn. **33**, 3391 (1997).
[12] T. L. Hylton *et al.,* Appl. Phys. Lett. **67**, 1154 (1995).
[13] J. A. Katine *et al.,* Appl. Phys. Lett. **76**, 354 (2000); K. Bussman *et al.,* Appl. Phys. Lett. **75**, 2476 (1999).
[14] S. K. Upadhyay *et al.,* Phys. Rev. Lett. **81**, 3247 (1998).
[15] F. Schreiber *et al.,* Solid State Commun. **93**, 965 (1995).
[16] J. Slonczewski, J. Magn. Magn. Mater. **195**, L261 (1999).
[17] H. B. Callen, J. Phys. Chem. Solids **4**, 256 (1958).